ISBN: 978-3-95450-231-8 ISSN: 2673-5490 doi: 10.18429/JACoW-IPAC2023-WEPL015

GENERALIZED GRADIENT FIELD DESCRIPTION USING THE BMAD AND PTC TOOLKITS

D. Sagan*†, E. Hamwi, Cornell University, Ithaca, NY, USA,
P. Nishikawa‡, KEK, Tsukuba, Japan

Abstract

The Generalized Gradient (GG) formalism of Venturini and Dragt [1] for describing static magnetic or electric fields has been implemented in the Bmad toolkit for accelerator simulations. In conjunction with this, a new method for calculating GG derivatives from a field table has been developed which avoids some of the problems of the Venturini and Dragt method. Generalized gradients are also implemented in the PTC toolkit developed by Étienne Forest which is interfaced to Bmad. This allows for construction of spin/orbital Taylor maps useful for nonlinear analysis and rapid tracking.

INTRODUCTION

Tracking particles through elements in an accelerator is fundamental to simulations. Standard techniques exist for tracking through fields that are longitudinally uniform. However, for elements with varying fields like an undulator or where the fringe fields are strong enough, tracking can be problematical both in terms of accuracy and speed. One way to handle complex static fields is with the Generalized Gradient (GG) description that was introduced by Venturini and Dragt [1, 2]. This formalism has been implemented into the Elegant program [3] and now has been implemented in the Bmad toolkit for accelerator simulations [4] as well as the PTC toolkit of Étienne Forest [5] that is integrated with Bmad. With PTC, spin/orbital Taylor maps can be computed from the GG description. The use of maps can decrease particle tracking times by orders of magnitude. Additionally, a map allows for the computation of many lattice parameters such as Twiss parameters, spin depolarization rates, higher order chromatic effects, etc.

Before GGs can be used in tracking, they must be calculated. Discussed in this paper is a new method for calculating GGs from a field table which avoids some of the problems of the Venturini and Dragt algorithm.

GG FIELD EQUATIONS

Following Venturini and Dragt [1], DC magnetic or electric fields can be described by a scalar potential

$$\mathbf{B} = -\nabla\,\psi_B, \qquad \mathbf{E} = -\nabla\,\psi_E \tag{1}$$

In cylindrical (ρ, θ, z) coordinates, the scalar potential ψ can be decomposed:

$$\psi = \sum_{m=1}^{\infty} \psi_{m,s}(\rho, z)\ \sin(m\theta) + \sum_{m=0}^{\infty} \psi_{m,c}(\rho, z)\ \cos(m\theta) \tag{2}$$

The $\psi_{m,\alpha}$ $(\alpha = c, s)$ can be expanded in powers of ρ:[1]

$$\psi_{m,\alpha} = \sum_{n=0}^{\infty} \frac{(-1)^{n+1} m!}{4^n\, n!\, (n+m)!}\, \rho^{2n+m}\, C^{[2n]}_{m,\alpha}(z) \tag{3}$$

where superscript $[j]$ indicates the j^{th} derivative of $C_{m,\alpha}(z)$. "Generalized gradients" are the name Venturini and Dragt gave to the functions $C_{m,\alpha}(z)$.

From the above equations, the field[2] is given by

$$\begin{aligned}
B_\rho &= \sum_{m=1}^{\infty}\sum_{n=0}^{\infty} \frac{(-1)^n\, m!\, (2n+m)}{4^n\, n!\, (n+m)!}\, \rho^{2n+m-1} \times \\
&\qquad \left[C^{[2n]}_{m,s}(z)\ \sin m\theta + C^{[2n]}_{m,c}(z)\ \cos m\theta\right] + \\
&\qquad\qquad \sum_{n=1}^{\infty} \frac{(-1)^n\, 2n}{4^n n!\, n!}\, \rho^{2n-1}\, C^{[2n]}_{0,c}(z) \\
B_\theta &= \sum_{m=1}^{\infty}\sum_{n=0}^{\infty} \frac{(-1)^n\, m!\, m}{4^n\, n!\, (n+m)!}\, \rho^{2n+m-1} \times \\
&\qquad \left[C^{[2n]}_{m,s}(z)\ \cos m\theta - C^{[2n]}_{m,c}(z)\ \sin m\theta\right] \\
B_z &= \sum_{m=0}^{\infty}\sum_{n=0}^{\infty} \frac{(-1)^n\, m!}{4^n\, n!\, (n+m)!}\, \rho^{2n+m} \times \\
&\qquad \left[C^{[2n+1]}_{m,s}(z)\ \sin m\theta + C^{[2n+1]}_{m,c}(z)\ \cos m\theta\right]
\end{aligned} \tag{4}$$

While the scalar potential only involves even derivatives of $C_{m,\alpha}$, the field itself is dependent upon all derivatives. The multipole index m is such that $m = 0$ is for solenoidal fields, $m = 1$ is for dipole fields, $m = 2$ is for quadrupolar fields, etc. The sine–like GGs represent normal (non-skew) fields and the cosine–like GGs represent skew fields.

The functions $C_{m,\alpha}(z)$ are characterized by specifying $C_{m,\alpha}(z_i)$ and derivatives at a set of longitudinal points z_i, up to some maximum derivative order $N_{m,\alpha}$ chosen by the user. The points z_i do not have to be equally spaced.

The advantage of a GG map over a cylindrical or Cartesian map decomposition [6, 7] come from the fact that the field at any point (x, y, z) is only dependent upon the $C^{[n]}_{m,\alpha}(z)$ at z and, by interpolation, the $C^{[n]}_{m,\alpha}(z)$ can be very well approximated using the $C^{[n]}_{m,\alpha}(z)$ values at the evaluation points z_i and z_{i+1} with z being in the interval $[z_i, z_{i+1}]$. This is in contrast to the cylindrical or Cartesian map decomposition

* david.sagan@cornell.edu
† Work supported in part by Department of Energy grant DE-SC0018370 and National Science Foundation award DMR-1829070.
‡ patrice.nishikawa@kek.jp

[1] Compared to Venturini and Dragt, a negative sign is introduced in Eqs. (1) and (3) to keep ψ_E consistent with the normal definition.

[2] For compactness, only the magnetic field will be considered. The description of the electric field is similar.

ISBN: 978-3-95450-231-8 ISSN: 2673-5490 doi: 10.18429/JACoW-IPAC2023-WEPL015

where the field at any point is dependent upon *all* of the terms that characterize the field. This "locality" property of generalized gradients means that calculating coefficients is easier (the calculation of $C_{m,\alpha}(z)$ at z_i can be done using only the field near z_i independent of other regions) and it is easier to ensure that the field goes to zero at the longitudinal ends of the element which avoids unphysical edge effects in tracking. Additionally, the evaluation is faster since only coefficients to either side of the evaluation point contribute. The disadvantage of generalized gradients is that since the derivatives are truncated at some order $N_{m,\alpha}$, the resulting field does not satisfy Maxwell's equations with the error as a function of radius scaling with the power $\rho^{m+N_{m,\alpha}}$.

GG FITTING

Before the GG field description can be used for particle tracking, the GG derivatives must be calculated. The method developed by Venturini and Dragt [1] starts with the radial field $B_\rho(R,\theta,z)$ at radius $\rho = R$. This field may be calculated from say, an electromagnetic field modeling program, or may be obtained from a measurement. The radial field may be expressed in terms of two sets of functions $B_m(R,z)$ and $A_m(R,z)$:

$$B_\rho(R,\theta,z) = \sum_{m=1}^{\infty} B_m(R,z)\,\sin(m\phi) + A_m(R,z)\cos(m\phi) \tag{5}$$

The GG derivatives can then be computed from the Fourier transforms of A_m and B_m. For B_m the equation is:

$$C^{[n]}_{m,s}(z) = \frac{i^n}{2^m\, m!}\frac{1}{\sqrt{2\pi}}\int_{-\infty}^{\infty} dk\, e^{ikz}\frac{k^{m+n-1}}{I'_m(kR)}\widetilde{B}_M(R,k) \tag{6}$$

where I_m is the modified Bessel function of the first kind and $\widetilde{B}_m$ is the Fourier transform of B_m

$$\widetilde{B}_m(R,k) = \frac{1}{\sqrt{2\pi}}\int_{-\infty}^{\infty} dz\, e^{-ikz}B_m(R,z) \tag{7}$$

Similarly, $C^{[n]}_{m,c}(z)$ can be expressed in terms of A_m. Borland, et. al [3] have developed comparable equations for the case where the field is known on a cylinder of rectangular cross-section.

In order to achieve higher accuracy, an alternative algorithm has been developed for use with Bmad. This "Bmad" algorithm takes advantage of the locality property of GGs and only field values near a given z_i are used to evaluate the $C^{[n]}_{m,\alpha}(z_i)$. The local nature of the Bmad method is in contrast to the non-local nature of the Venturini and Dragt algorithm which uses an integration of the field on the entire cylinder surface. With the Bmad method, in regions of low field, the calculation is not "polluted" by having to integrate over regions of relatively high field. At the ends of the element where deviations from zero can lead to unphysical edge field effects, this can be a concern. Another difference is that the Bmad algorithm can use known field values on an arbitrary grid of points and is not limited to cylindrical surfaces. In fact, the algorithm works best with grid points throughout the entire element volume.

With the Bmad algorithm, at any evaluation point z_i, the GG derivatives are fit to the set of field data points that are within some region $[z_i - \delta z, z_i + \delta z]$ where δz is set by the user. At any field point $\mathbf{r} = (x,y,z)$, the GG derivatives at z, up to the truncation order $N_{m,\alpha}$, are calculated by extrapolation from the GG derivatives at z_i via

$$C^{[n]}_{m,\alpha}(z) = \sum_{j=n}^{N_{m,\alpha}} \frac{(z-z_i)^{j-n}}{(j-n)!}\, C^{[j]}_{m,\alpha}(z_i) \tag{8}$$

From the $C^{[n]}_{m,\alpha}(z)$, the field at $\mathbf{r}$ can be calculated from Eqs. (4). From Eqs. (4) and (8), it is seen that the field at any point is linearly dependent upon the $C^{[n]}_{m,\alpha}(z_i)$. It is thus straightforward to calculate a best fit set of GG derivatives at z_i that minimize the merit function M

$$M = \sum_k W_k \left|\mathbf{B}_{\rm fit}(\mathbf{r}_k) - \mathbf{B}_{\rm k,grid}\right|^2 \tag{9}$$

where k is an index that runs over the set of field points used in the fit, W_k is a weighting function, $\mathbf{B}_{\rm k,grid}$ is the field that is fit to at point $\mathbf{r}_k$, and $\mathbf{B}_{\rm fit}(\mathbf{r}_k)$ is the field as calculated from the GGs at point z_i via Eq. (8).

The derivative order cut-offs $N_{m,\alpha}$ can be varied to find values such that the derivatives beyond the cut-offs are not significant. One strategy is to choose $N_{m,\alpha} = N_e - m$ where N_e is some fixed integer and the m used in the fit are limited to be $m \le N_e$. With this choice, the variation in field as a function of radius is capped at ρ^{N_e-1} for all m (see Eqs. (4)).

The larger the range of δz used for evaluating the derivatives, the smoother the derivatives from one z_i to the next will be. However, the range should not be so large that the polynomial extrapolation (Eq. (8)) is inaccurate.

Generally it is the "core" field near the $x = y = 0$ axis that needs to be well fit for tracking purposes. To get a better core fit, the weight of the core field points can be increased over points further out. The Bmad fitting program uses a weight of

$$W_k = \frac{R^2_{\rm max}}{R^2_{\rm max} + (w_c - 1)\,(x_k^2 + y_k^2)} \tag{10}$$

where w_c is a user settable constant and $R^2_{\rm max} = \max_k(x_k^2 + y_k^2)$ with the k index running over all field points. Setting $w_c = 1$ gives a uniform weighting and increasing w_c gives more weight to the core points.

IMPLEMENTATION IN BMAD AND PTC

Particle tracking through fields defined by GGs is done in Bmad using Runge-Kutta integration. Interpolation of the field is done by constructing an interpolating polynomial of order $2N_{m,\alpha} + 1$ for each interval $[z_i, z_{i+1}]$ which has the correct derivatives from 0 to $N_{m,\alpha}$ at points z_i and z_{i+1}. The coefficients of the interpolating polynomial are easily calculated by inverting the appropriate matrix equation. The coefficients of the interpolating polynomial are

ISBN: 978-3-95450-231-8 ISSN: 2673-5490 doi: 10.18429/JACoW-IPAC2023-WEPL015

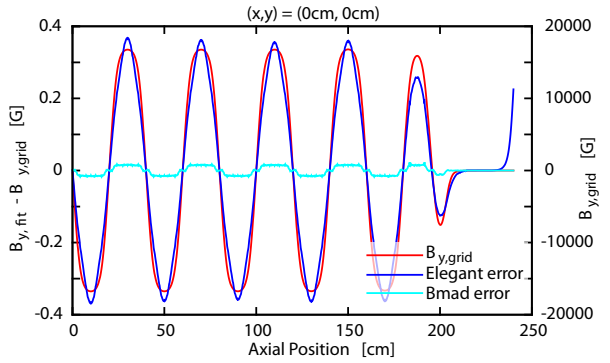

Figure 1: Vertical field B_y along the center line $(x, y) = (0, 0)$. Since the field is anti-symmetric, only half the field is shown. Plotted is the field as given by the field grid, $B_{y,\mathrm{grid}}$ (red curve), along with the difference between this field and the fit field $B_{y,\mathrm{fit}}$ calculated from the GGs as calculated by the Elegant method (blue curve) and the Bmad algorithm (cyan curve).

calculated and stored before tracking to avoid evaluation of the coefficients during tracking.

The PTC toolkit[5] developed by Étienne Forest is interfaced to Bmad. The analytic nature of the GG description allows PTC to construct a corresponding spin/orbital Taylor map. The utilization of maps not only leads to a large decrease in computation time but also facilitates the use of such maps for normal form analysis. This enables the computation of various parameters, including, but not limited to, Twiss parameters, spin depolarization rates, and higher order chromatic effects.

WIGGLER FIELD EXAMPLE

The new GG fitting procedure was tested with a 4.2 meter long 21 pole wiggler. The field data was calculated by an electromagnetic field solver. Field data was generated in a grid 0.4 cm × 0.2 cm × 0.2 cm between points in x, y, and z respectively. The extent of the field data was ±5.2 cm × ±2.6 cm × 4.8 m in x, y, and z.

GG derivatives were computed using both the Elegant and Bmad fitting algorithms. Due to the symmetry of the field, only sine-like GGs are needed. A good fit was obtained using five GGs with $m = 1, 3, 5, 7,$ and 9 and with a varying derivative cutoff of $N_{m,s} = 10 - m$. GG derivatives were computed in z every 0.2 cm corresponding to the granularity of the field table.

For the Bmad algorithm, a good fit was produced with the longitudinal range of field points δz set to 0.4 cm corresponding to using 5 planes of data for each fit at a given z_i position (except at the ends which used 3 fit planes and the neighboring end points use 4 fit planes). Additionally, a weight w_c of 10^3 produced good fits both near the center line and at the periphery of the grid. These values were used to fit the GGs used in creating the plots shown.

Figure 1 shows the vertical field B_y along the center line $(x, y) = (0, 0)$. Plotted is the field $B_{y,\mathrm{grid}}$ as given by the field grid along with the difference between this field and the fit field calculated from the GG derivatives as derived by the Elegant and Bmad algorithms. The RMS of the difference $|\mathbf{B}_{\mathrm{grid}} - \mathbf{B}_{\mathrm{fit}}|$ between grid and fit is 0.012 Gauss for the Bmad fit and 0.22 Gauss for the Elegant fit. This is to be compared to an RMS of 12000 for the field $\mathbf{B}_{\mathrm{grid}}$ itself. The Bmad fit achieves an accuracy of 1 part in 10^6 and is about a factor of 20 better than the Elegant fit.

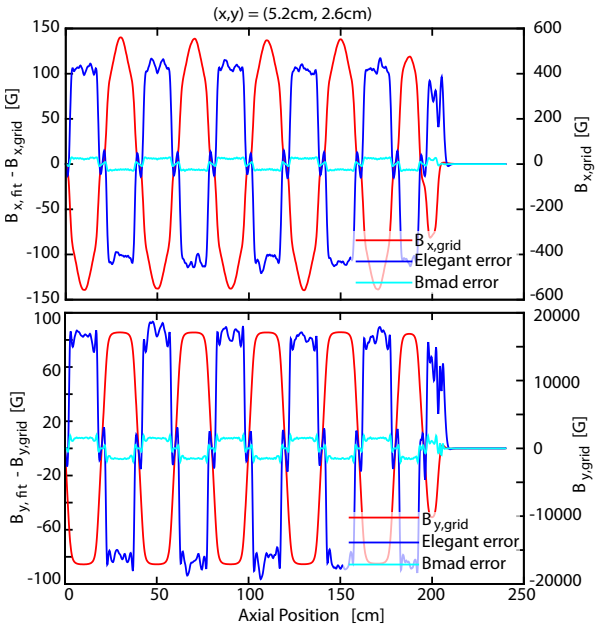

Figure 2: Same as Fig. 1 except data is drawn for the line at maximal grid radius $(x, y) = (5.2\mathrm{cm}, 2.6\mathrm{cm})$. Top: Horizontal B_x component. Bottom: Vertical B_y component.

Figure 2 shows the same thing as Fig. 1 for B_y and B_x with the field evaluated at the edge of the field grid at $(x, y) = (5.2\mathrm{cm}, 2.6\mathrm{cm})$. Here the RMS of the difference $|\mathbf{B}_{\mathrm{grid}} - \mathbf{B}_{\mathrm{fit}}|$ is good but not as stellar as on the center line. For the Bmad fit the RMS is 8 Gauss, which is about 1 part in 3500 compared to an RMS of 14500 for the field $\mathbf{B}_{\mathrm{grid}}$ itself. For the Elegant fit, the RMS is 110 Gauss. The Bmad fit is over a factor of 10 better than the Elegant fit.

CONCLUSION

The generalized gradient formalism has been integrated with the Bmad and PTC toolkits allowing for the construction of truncated Taylor series maps that can be used for analysis and fast tracking. In conjunction with this, a new GG derivative fitting algorithm has been developed which can be used to accurately calculate GG coefficients.

ACKNOWLEDGMENTS

Thanks to Ryan Lindberg and Michael Borland for generating the GG derivatives using Elegant and for useful discussions.

ISBN: 978-3-95450-231-8 ISSN: 2673-5490 doi: 10.18429/JACoW-IPAC2023-WEPL015

REFERENCES

[1] M. Venturini and A. J. Dragt, "Accurate computation of transfer maps from magnetic field data," *Nucl. Instrum. Methods Phys. Res., Sect. A*, vol. 427, no. 1-2, pp. 387–392, 1999.

[2] M. Venturini, D. Abell, and A. Dragt, "Map computation from magnetic field data and application to the lhc high-gradient quadrupoles," *Proc. of the 5th Intern. Computational Accelerator Physics Conference*, pp. 184–188, 1998.

[3] M. Borland, R. R. Lindberg, R. Soliday, and A. Xiao, "Tools for Use of Generalized Gradient Expansions in Accelerator Simulations," in *Proc. IPAC'21*, Campinas, Brazil, May 2021, pp. 253–256. doi:10.18429/JACoW-IPAC2021-MOPAB059

[4] D. Sagan, "Bmad: A relativistic charged particle simulation library," *Nucl. Instrum. Methods Phys. Res., Sect. A*, vol. 558, no. 1, pp. 356–359, 2006.

[5] F. Schmidt, E. Forest, and E. McIntosh, "Introduction to the polymorphic tracking code: Fibre bundles, polymorphic Taylor types and "Exact tracking"," CERN, Tech. Rep. CERN-SL-2002-044-AP, KEK-REPORT-2002-3, 2002. http://cds.cern.ch/record/573082

[6] A. Wolski, "Maxwell's equations for magnets," *arXiv preprint arXiv:1103.0713*, 2019.

[7] D. Sagan, J. Crittenden, D. Rubin, and E. Forest, "A magnetic field model for wigglers and undulators," in *Proceedings of the 2003 Particle Accelerator Conference*, IEEE, vol. 2, 2003, pp. 1023–1025.